PII: S0032-3861(97)00588-0

Polymer Vol. 39 No. 12, pp. 2563–2569, 1998
© 1998 Elsevier Science Ltd
Printed in Great Britain. All rights reserved
0032-3861/98/$19.00+0.00

Thermomechanical behaviour of semicrystalline polymers submitted to plane-strain compression

Irene T. S. Garcia and Dimitrios Samios*
Instituto de Química, Universidade Federal do Rio Grande do Sul, Cx. Postal 15003, 91501-970, Porto Alegre/RS, Brazil

(Received 27 March 1997; revised 28 May 1997)

High-density polyethylene (HDPE) and poly(vinylidene fluoride) (PVF_2) were submitted to plane-strain compression at temperatures between the glass transition temperature (T_g) and the melting point (T_m) by using a deep channel die; this device allowed compression along the Z-axis, elongation along the X-axis and no dimensional change along the Y-axis. The thermomechanical and morphological changes occurring during the plastic deformation process and relaxation of the deformed materials were investigated by thermomechanical analysis, differential scanning calorimetry and density measurements. The results show that the deformation process affects the thermodynamic properties of polymers, introducing different characteristics into the material. An increase of amorphous phase was registered in both materials. The plastically deformed semicrystalline polymers showed non-regular linear thermal expansion behaviour in the deformation directions (X and Z). The relaxation process, which is obtained by heating the deformed materials, is characterized by 'shape and temperature memory'. © 1998 Elsevier Science Ltd. All rights reserved.

(Keywords: semicrystalline polymers; memory; deformation)

INTRODUCTION

Semicrystalline polymer systems can be modified through the application of a well-defined axial compression in the temperature range between the glass transition temperature, T_g, and the melting point, T_m.

Morphological changes in semicrystalline polymers during stress application have been studied by Flory[1] and Peterlin[2]; Flory proposed that plastic deformation occurs by fusion and recrystallization of the crystal phase present in the semicrystalline polymer and Peterlin added the so-called 'micronecking mechanism'. Recently, Barctzack, Cohen and Argon[3] have studied plastic deformation mechanisms by submitting high-density polyethylene (HDPE) to uniaxial deformation at room temperature and identified chain slip as the active deformation mechanism. Argon *et al.*[4–8] studied textured polymers, Nylon 6, poly(ethylene terephthalate) and HDPE, obtained by plane-strain compression near their respective melting points, characterizing the mechanical and morphological modifications of the materials.

The 'shape memory' effect in deformed materials, which has been studied extensively since it was observed in Au–Cd alloys by Ölander[9], has been observed in semicrystalline polymer materials. In spite of the industrial and medical applicability[10,11] of this phenomenon, there are still only a few products with successful industrial uses. It is generally accepted[12] that theoretical and experimental studies of the recovery mechanisms of deformed polymers need more attention.

Several studies concerned with the shape 'memory' aspects of semicrystalline polymers deformed by axial compression[13,14] and plane-strain compression[15], have detected another kind of memory behaviour during the thermal cycles following deformation. The deformed semicrystalline polymers demonstrated a 'memory' of the last highest achieved temperature (HAT) during the different thermal cycles.

The aim of this work was to establish the relationship between deformation directions and thermomechanical properties as well as the recuperation process. The use of a deep channel die allowed the application of plane-strain compression at room temperature to the poly(vinylidene fluoride) (PVF_2) and HDPE studied in this work. The deformed materials have been studied with respect to the three different deformation directions by means of thermomechanical analysis (t.m.a.) techniques. Melting enthalpies as well as density measurements on the deformed and undeformed materials provided information about the crystallinity.

EXPERIMENTAL

Two semicrystalline polymers were studied: HDPE (Polialden Company, $\bar{M}_n = 18\,000\ \mathrm{g\ mol^{-1}}$ and $\bar{M}_w = 280\,000\ \mathrm{g\ mol^{-1}}$) and PVF_2 (Pennwalt Corporation, $\bar{M}_n = 59\,000\ \mathrm{g\ mol^{-1}}$ and $\bar{M}_w = 370\,000\ \mathrm{g\ mol^{-1}}$). These polymers were submitted to plane-strain compression over a range of pressures that does not produce microcracking. The samples were characterized by thermomechanical analysis, differential scanning calorimetry (d.s.c.), densimetry and plastic deformation measurements.

Sample preparation

The sample preparation was carried out in three stages:

---

* To whom correspondence should be addressed

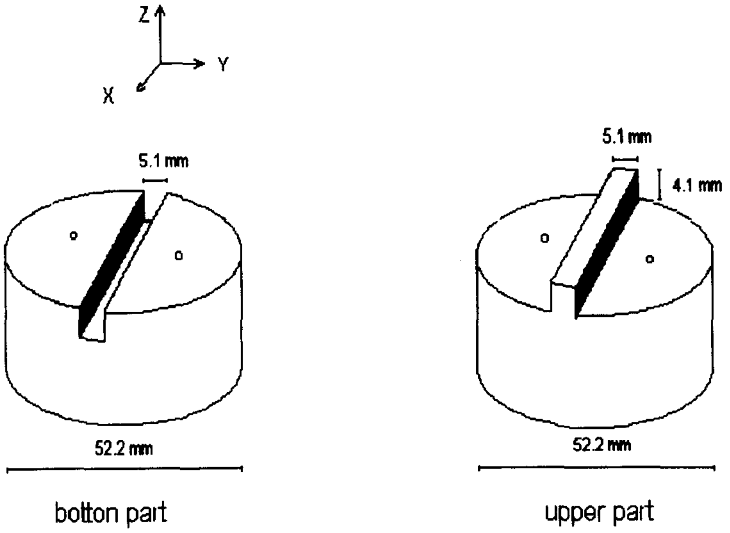

Figure 1 Deep channel die used to carry out the plane-strain compression

preparation of 2 mm thick plates, cutting into the desired dimensions for each experiment, and heating near the respective melting point in order to eliminate the stress generated during the processing.

Fabrication of the plates was carried out by moulding polymer pellets at 150°C for HDPE and 180°C for PVF_2, at a moulding pressure of 3 MPa for both polymers. Afterwards, samples were cut to the desired shape and smoothed with a 600 grit sandpaper. Stress elimination was carried out by heating to temperatures below the melting point of the polymers (110°C for HDPE and 145°C for PVF_2) and slow cooling back to room temperature (2°C min^{-1}). Samples were deformed in a deep channel die (*Figure 1*) which allowed a compression along the *Z*-axis and expansion along the *X*-axis, whereas the dimension along the *Y*-axis remained the same. The hydraulic press enabled the applied pressure to be raised from zero to defined value between zero and 1110 MPa. The pressure rise rate was approximately 185 MPa s^{-1}, which permitted very fast elevation of the sample pressure to the desired value. The sample was maintained under pressure for 10 s and then the pressure was released. This procedure was performed at 25 ± 2°C.

Plastic deformation

The plastic deformation was studied in the range of pressure from 0 to 925 MPa for HDPE and from 0 to 1110 MPa for PVF_2. The measurements of sample dimensions, before and 1 h after deformation, were carried out with a micrometer. The percentage plastic deformation was determined as the ratio between deformation and initial dimension:

$$D = \frac{l_f - l_i}{l_i} \times 100 \qquad (1)$$

where l_f is the final sample dimension and l_i is the initial one. Measurements for each pressure applied were repeated on three different samples and results are expressed as the average values of these measurements.

Thermomechanical analysis

The linear thermal expansion behaviour at the three deformation coordinate axes was evaluated by t.m.a. The procedure consisted of scanning consecutive thermal cycles in a Perkin–Elmer Thermal Analyzer, each cycle starting by raising the temperature to the greatest value of the cycle followed by cooling down to the initial value in an atmosphere of dry N_2 gas. The upper temperature value of each cycle was chosen in order to obtain a sufficient number of cycles to permit characterization of the material's thermal behaviour before it melted. The thermal linear expansion behaviour with temperature for each deformation direction was registered.

For HDPE the lower temperature of the cycles was 40°C and the upper temperatures of the consecutive cycles were 55, 70, 85 and 100°C. For PVF_2 the lower temperature of the cycles was 40°C and the upper temperatures were 70, 90, 110 and 130°C. The temperature scanning rate was 5°C min^{-1} and an unloaded t.m.a. expansion probe was used.

Differential scanning calorimetry and densimetry determination

The degree of crystallinity, defined as the ratio between ΔH_M and ΔH_0 where ΔH_M is the melting enthalpy of the material under study and ΔH_0 the melting enthalpy of totally crystalline material, was determined in a DSC-4 Perkin–Elmer instrument. ΔH_0 is 286.58 J g^{-1} for HDPE[16] and 104.50 J g^{-1} for PVF_2[17].

The density of the samples, before and after deformation, was determined by the standard hydrostatic method at 25±2°C.

RESULTS AND DISCUSSION

The plastic deformation behaviour with applied pressure along the three deformation axes is shown in *Figures 2 and 3* for HDPE and PVF_2, respectively. As far as pressure is concerned, three characteristic regions can be observed. With respect to the *Z* and *X* deformation axes, both figures show a small initial region characterized by linear deformation behaviour, followed by a non-linear behaviour which is the main deformation region, and finally a saturation region characterized by constant deformation with increasing pressure. The main deformation region of HDPE begins near 50 MPa, whereas the same region in PVF_2 begins after 100 MPa. From the saturation regions it can be seen that the pressure at the beginning of saturation is lower for HDPE than for PVF_2. The saturation pressure

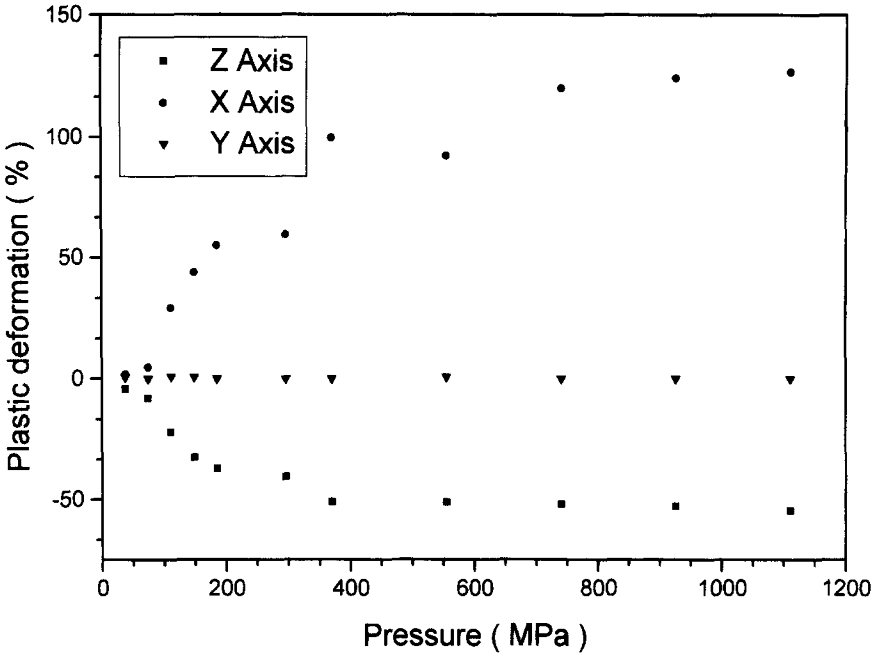

Figure 2 Percentage plastic deformation of HDPE along the three deformation axes

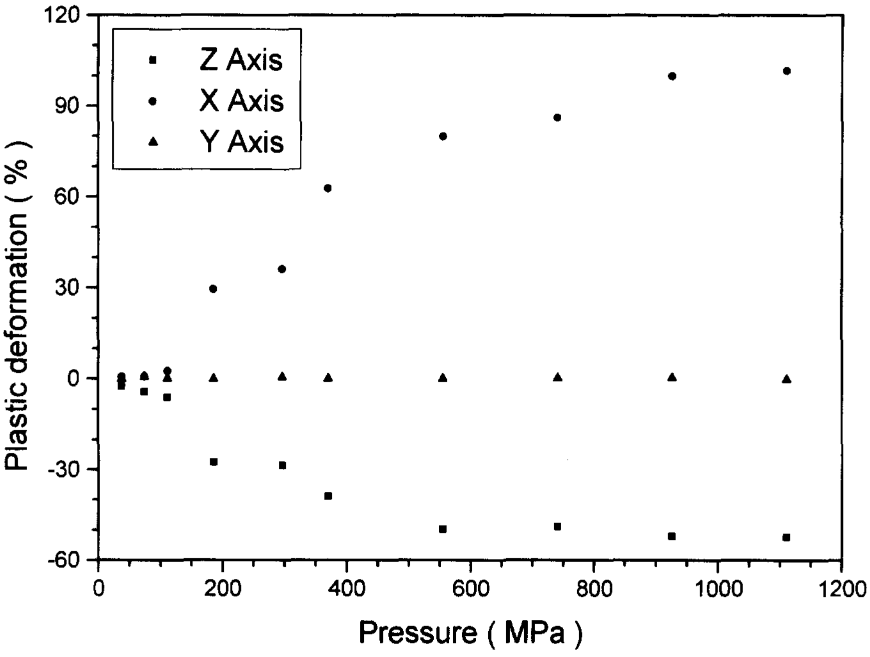

Figure 3 Percentage plastic deformation of PVF_2 along the three deformation axes

values, P, are: Z-axis—$P_{HDPE} = 350$ MPa, $P_{PVF2} = 550$ MPa; X-axis—$P_{HDPE} = 750$ MPa, $P_{PVF2} = 950$ MPa. The other aspect that can be discussed from *Figures 2 and 3* is the percentage deformation in the saturation region. The percentage deformation values at saturation region, PD, are: Z-axis—$PD_{HDPE} = 60\%$, $PD_{PVF2} = 50\%$; X-axis—$PD_{HDPE} = 135\%$, $PD_{PVF2} = 100\%$. The plastic deformation aspects of the HDPE and PVF_2 are related to their structural and morphological characteristics. HDPE demonstrates a higher plastic deformation capability compared with PVF_2. As will be seen later, this aspect is additionally related to the thermomechanical memory behaviour of the studied materials.

Thermomechanical analysis scans through four thermal scanning cycles for undeformed and deformed HDPE are shown in *Figures 4 and 5*, respectively. The behaviour of the thermal expansion along the three orthogonal directions (Z, X, Y) can be seen. Undeformed material exhibits isotropic expansion behaviour along the three axes, whereas deformed material demonstrates a well-defined anysotropic behaviour. The deformed material shows accentuated thermal response along the directions where plastic deformation occurred; every thermal scanning curve is composed of an initial normal expansion followed by a strong expansion or strong shrinkage response depending on the deformation axis: strong shrinkage along the X-axis, strong expansion along the Z-axis and a very small shrinkage along the Y-axis (probably originated by a small

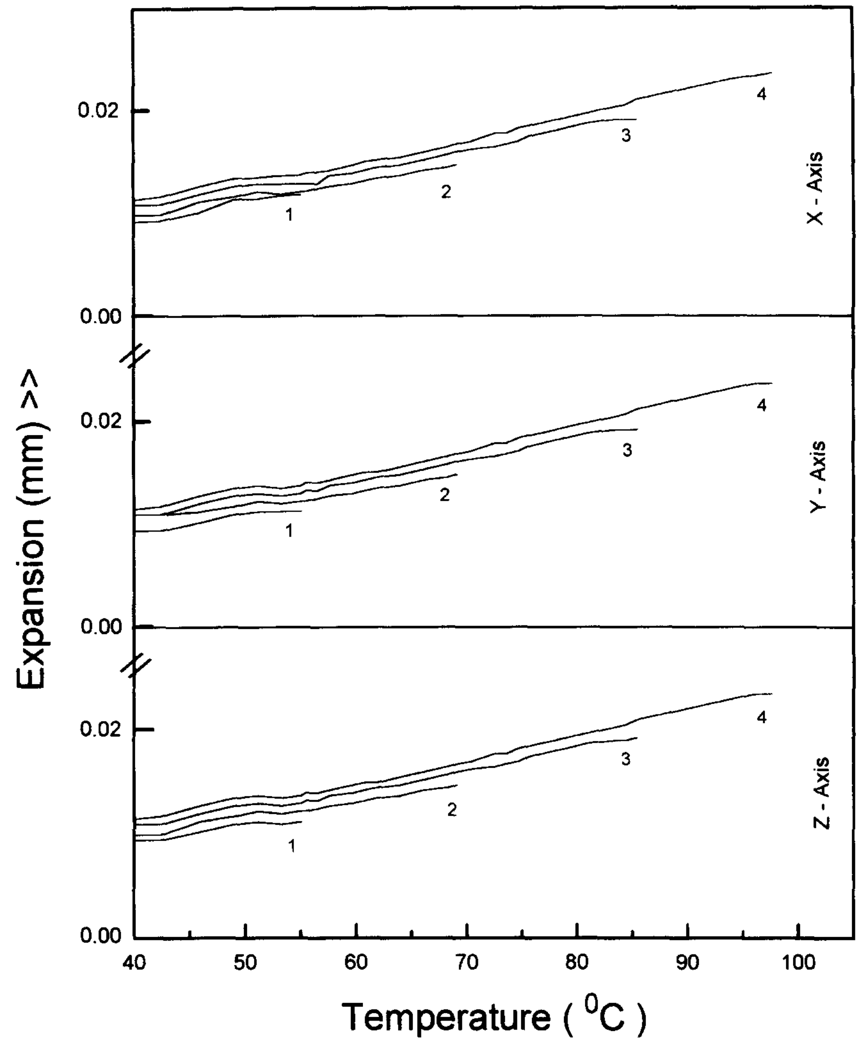

Figure 4 Thermal expansion of undeformed HDPE along the three orthogonal axes, *X*, *Y* and *Z*. Heating cycles: (1) 40–55°C; (2) 40–70°C; (3) 40–85°C; (4) 40–100°C. Scanning rate: 5°C min^{-1}

deformation along the *Y*-axis). Similar behaviour was observed for PVF_2. The linear thermal expansion coefficients, obtained during the scanning cycles, are represented by α_{lik}, where l is the deformation axis (Z, X or Y), i is the number of the heating cycle (1, 2, 3 or 4) and k shows that the temperature range where the expansion coefficient is measured is below ($k = 1$) or above ($k = 2$) the last highest achieved temperature (see, for instance, in *Figure 5* the location of α_{X12}, α_{X21}, α_{X22}). The linear thermal expansion coefficients for undeformed and deformed HDPE are listed in *Table 1* and *Table 2* respectively, while those for undeformed and deformed PVF_2 are given in *Table 3* and *Table 4* respectively. Both undeformed polymers show average α_{lik} values of approximately $2 \times 10^{-4}\,°C^{-1}$. In every thermal cycle, the deformed materials demonstrate a low or normal absolute average values of α_{li1}. The average α_{li1} values for HDPE are: $\alpha_{Zi1} = 3.5 \times 10^{-4}\,°C^{-1}$, $\alpha_{Xi1} = 0°C^{-1}$; the corresponding PVF_2 α_{li1} values are: $\alpha_{Zi1} = 4 \times 10^{-4}\,°C^{-1}$, $\alpha_{Xi1} = 0°C^{-1}$. The absolute average values of α_{li2}, in other words the expansion coefficients in the region above the last highest achieved temperature, are much higher than those obtained in the relaxed materials. The average α_{li2} values for HDPE are: $\alpha_{Zi2} = 20 \times 10^{-4}\,°C^{-1}$, $\alpha_{Xi2} = -13 \times 10^{-4}\,°C^{-1}$; for PVF_2 the average α_{li2} values are: $\alpha_{Zi2} = 38 \times 10^{-4}\,°C^{-1}$, $\alpha_{Xi2} = -26 \times 10^{-4}\,°C^{-1}$.

The analysis of these results shows the existence of two kind of 'memory' in the material: the well-known 'shape memory' and the 'temperature memory' which was detected in all directions where a deformation was introduced. The terms 'temperature memory' and 'shape memory' are introduced as equivalent to 'thermomechanical memory', which has been used in previous works[13–15]. The 'temperature memory' is defined here as the characteristic behaviour of the deformed material 'to remember', during a heating procedure, the highest achieved temperature in the previous heating cycle (HAT). These temperatures (HAT) are located at the points where the expansivity shows a very accentuated change (see *Figure 5*). The plane-strain compression technique permitted us to observe that this effect occurs not only along the direction of the applied pressure[13], but in all directions where deformation is verified. A comparison of the obtained α_{lik} values reveals that deformed HDPE has a lower tendency to recover its original shape than PVF_2. This characteristic property of the materials studied is in agreement with the higher plastic deformation capability obtained for the HDPE compared with PVF_2.

The d.s.c. data of undeformed and deformed materials are shown in *Figures 6 and 7* for HDPE and PVF_2, respectively. A slight decrease in melting temperature with increasing pressure is verified in the HDPE samples. As can be seen in

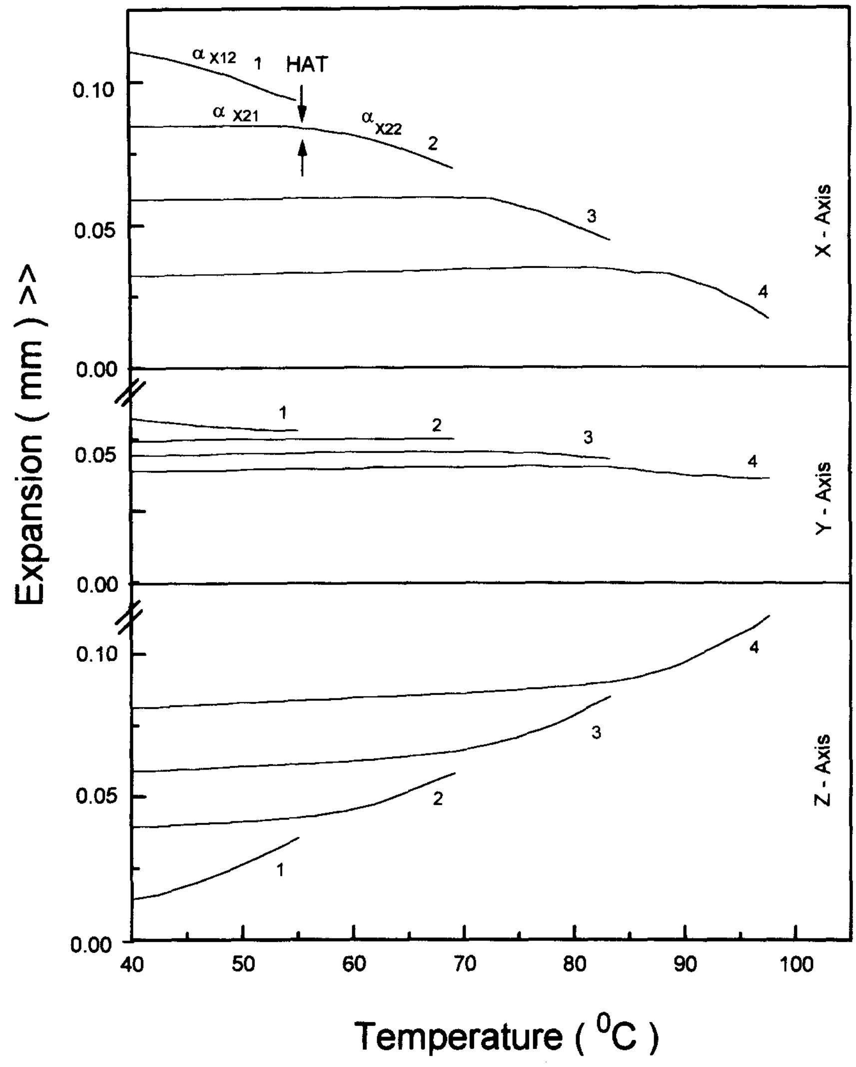

Figure 5 Thermal expansion of HDPE along the three orthogonal axes by applying 370 MPa. Heating cycles: (1) 40–55°C; (2) 40–70°C; (3) 40–85°C; (4) 40–100°C. Scanning rate: 5°C min^{-1}

Table 1 Linear thermal expansion coefficients of undeformed HDPE, along the three orthogonal axes, in different scanning cycles

Scanning cycle		α_{lik} (10^{-4} °C^{-1})					
		Z-axis		*X*-axis		*Y*-axis	
i	°C	α_{Zi1}	α_{Zi2}	α_{Xi1}	α_{Xi2}	α_{Yi1}	α_{Yi2}
1	40–55	—	1.0	—	1.2		1.5
2	40–70	1.4	1.1	1.3	1.5	1.4	1.1
3	40–85	2.1	2.4	2.3	2.4	2.0	2.0
4	40–100	2.4	3.1	2.4	2.9	2.0	3.2

Table 2 Linear thermal expansion coefficients of deformed HDPE, along the three orthogonal axes, in different scanning cycles. The applied pressure is 370 MPa

Scanning cycle		α_{lik} (10^{-4} °C^{-1})					
		Z-axis		*X*-axis		*Y*-axis	
i	°C	α_{Zi1}	α_{Zi2}	α_{Xi1}	α_{Xi2}	α_{Yi1}	α_{Yi2}
1	40–55	—	22.8	—	− 12.4	—	− 2.9
2	40–70	3.2	16.0	0.0	− 10.8	0.3	− 0.3
3	40–85	4.0	18.1	0.0	− 12.8	0.5	− 1.6
4	40–100	3.4	23.7	0.0	− 14.8	0.3	− 3.2

Table 3 Linear thermal expansion coefficients of undeformed PVF$_2$, along the three orthogonal axes, in different scanning cycles

Scanning cycle		α_{lik} (10^{-4} °C^{-1})					
		Z-axis		*X*-axis		*Y*-axis	
i	°C	α_{Zi1}	α_{Zi2}	α_{Xi1}	α_{Xi2}	α_{Yi1}	α_{Yi2}
1	40–70	—	2.0	—	2.3	—	2.2
2	40–90	1.7	2.0	2.0	2.6	2.0	2.4
3	40–110	2.3	1.9	2.0	2.2	2.3	2.0
4	40–130	2.7	1.9	2.7	2.0	2.6	2.0

Table 4 Linear thermal expansion coefficients of deformed PVF$_2$, along the three orthogonal axes, in different scanning cycles. The applied pressure is 370 MPa

Scanning cycle		α_{lik} (10^{-4} °C^{-1})					
		Z-axis		*X*-axis		*Y*-axis	
i	°C	α_{Zi1}	α_{Zi2}	α_{Xi1}	α_{Xi2}	α_{Yi1}	α_{Yi2}
1	40–70	—	29.8	—	− 19.4	—	− 2.9
2	40–90	2.9	29.9	0.0	− 20.4	1.5	− 0.2
3	40–110	4.3	38.5	0.0	− 25.1	2.0	0.0
4	40–130	5.2	55.3	0.1	− 38.5	2.3	1.7

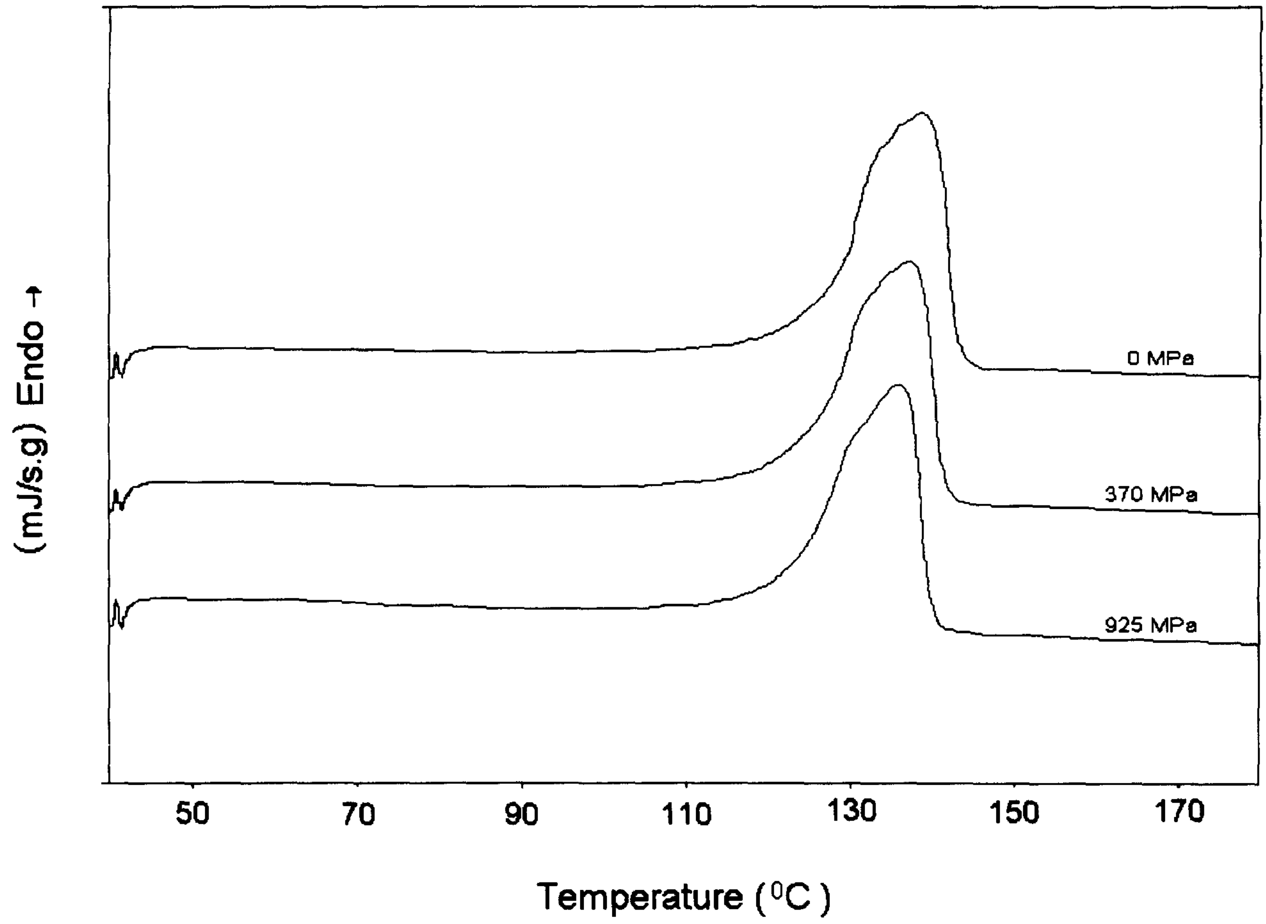

Figure 6 D.s.c. curves of HDPE at a heating rate of 10°C min^{-1}

Table 5 Melting enthalpy and degree of crystallinity for HDPE

Pressure (MPa)	T_m (°C)	Melting enthalpy ($J\ g^{-1}$)	Degree of crystallinity (%)
0	138.87	233.54	83
370	138.16	222.92	81
925	137.61	213.18	76

Table 6 Melting enthalpy and degree of crystallinity for PVF_2

Pressure (MPa)	T_m (°C)	Melting enthalpy ($J\ g^{-1}$)	Degree of crystallinity (%)
0	160.97	57.39	56
185	161.85	57.35	55
370	163.09	55.84	52
1110	163.3	51.99	50

Table 5, the melting enthalpy and consequently the degree of crystallinity of the HDPE studied here decreases with increasing applied deformation pressure. *Table 6* shows for PVF_2 a decreasing total melting enthalpy with increasing applied deformation pressure as in the case of HDPE; however, values of degree of crystallinity are smaller for PVF_2 than those obtained for HDPE.

An aspect deserving of further discussion is the shape of the PVF_2 thermograms. *Figure 7* shows that a significant change in the thermograms occurs with increasing applied deformation pressure. The melting thermogram of the undeformed PVF_2 samples includes an increase in specific heat (c_p) at 105°C which, according to Loufakis and Wunderlich, can be attributed to the melting of 'condis crystals'[18]. The main melting peak is composed of two superimposed peaks: one with a maximum situated at 147°C and the other at 161°C. The disappearance of the c_p discontinuity with increasing applied deformation pressure can be observed. By the same token, the melting peak originally situated at 147°C disappears and the peak originally situated at 161°C is shifted to higher values, showing that the applied deformation pressure preferentially affects the low-temperature crystals. Density measurements (*Table 7*) have shown a decrease in density with the applied pressure. This fact corroborates the melting enthalpy and the degree of crystallinity obtained through d.s.c. measurements.

CONCLUSIONS

Plane-strain compression applied in semicrystalline polymers, in the temperature range between the T_g and T_m, produces materials characterized by a non-equilibrium thermodynamic state. The observed plastic deformation values are higher for HDPE than for PVF_2. The recovery process, during the temperature elevation, is different along the three deformation axes for the deformed materials. The tendency to recover the original shape is more accentuated in PVF_2 than in HDPE. The degree of crystallinity of both polymers decreases with applied deformation pressure. A decrease in the HDPE melting temperature is observed with increasing of applied pressure, while for PVF_2 the melting

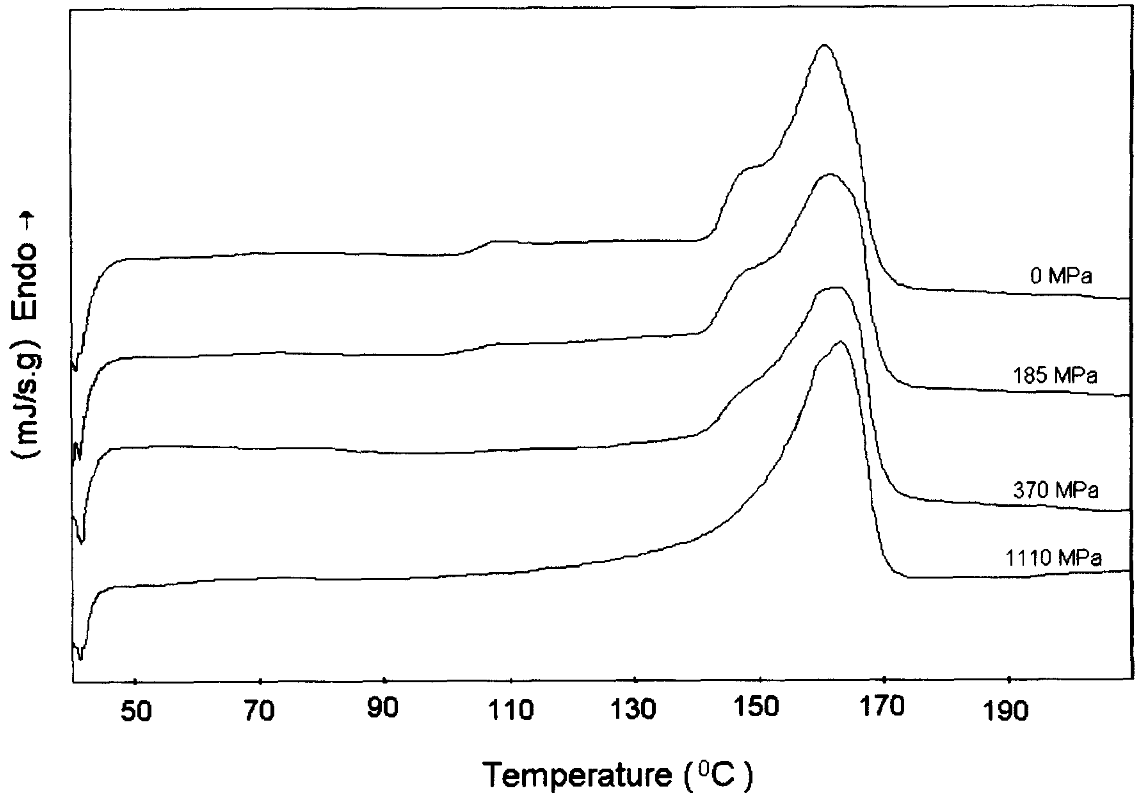

Figure 7 D.s.c. curves of PVF_2 at a heating rate of 10°C min^{-1}

Table 7 Density measurements at 25 ± 2°C for HDPE and PVF_2

Pressure (MPa)	Density (g cm^{-3})	
	HDPE	PVF_2
0	0.9627 ± 0.0020	1.7707 ± 0.0002
925	0.9593 ± 0.0003	—
1110	—	1.7689 ± 0.0006

temperature increases with applied pressure. In PVF_2, the low-temperature crystals are strongly affected by the applied pressure.

Both materials showed the memory temperature effect. At temperatures below HAT (high achieved temperarure), the material demonstrates apparently normal expansion behaviour. The shape recovery process of the deformed material is observed irreversibly in the region after HAT. This effect can be understood by assuming that the macromolecular mobility activation process, in the temperature range between T_g and T_m, is characterized by a wide activation energy distribution. Part of the energy gained during the temperature elevation of the deformed polymer is used for a partial structural recovering. This partial recovery is related to the part of the activation energy distribution responsible for the partial activation until the achieved temperature.

This experimental aspect of polymer behaviour may need to be considered during material processing (extrusion, moulding, etc.) in order to avoid future defects in polymer artefacts. Additionally, the memory behaviour indicates that these materials may find application as a 'one way' temperature sensor.

ACKNOWLEDGEMENTS

The authors are grateful to CAPES and CNPq for the financial support. The authors thank to Professor José Schifino and Maria Inez G. Miranda for their comments during preparation of the manuscript.

REFERENCES

1. Flory, P. J. and Yoon, D. Y., *Nature*, 1978, **272**, 226.
2. Peterlin, A., *J. Mater. Sci.*, 1971, **6**, 490.
3. Bartczac, Z., Cohen, R. C. and Argon, A. S., *Macromolecules*, 1992, **25**, 4692.
4. Lin, L. and Argon, A. S., *Macromolecules*, 1992, **25**, 4011.
5. Bartczac, Z., Argon, A. S. and Cohen, R. C., *Macromolecules*, 1992, **25**, 5036.
6. Galeski, A., Bartczac, Z., Argon, A. S. and Cohen, R. C., *Macromolecules*, 1992, **25**, 5705.
7. Bellare, A., Cohen, R. E. and Argon, A. S., *Polymer*, 1993, **34**, 1393.
8. Bartczac, Z., Argon, A. S. and Cohen, R. C., *Polymer*, 1994, **35**, 3427.
9. Ölander, A., *J. Am. Chem. Soc.*, 1932, **54**, 3819.
10. Banks, R., in *Shape Memory Effects in Alloys*, ed. J. Perkins. Plenum Press, New York, 1975, p. 537.
11. Filip, P., Musialek, J. and Manazec, K., *J. de Phys. IV*, 1995, **C8**, 1211.
12. Gillet, Y., Meunier, M. A., Brailovski, V., Trochu, F., Patoor, E. and Berveiller, M., *J. de Phys. IV*, 1995, **C8**, 1165.
13. Lima, M. F. S., Samios, D. and Villetti, M., *J. Polym. Eng.*, 1997, **17**, 75.
14. Samios, D. and Lima, M. F. S., *J. Polym. Eng.*, 1997, **17**, 139.
15. Garcia, I. T. S., M.Sc. thesis, Universidade Federal do Rio Grande do Sul, 1995.
16. Pae, K. D., *J. Polym. Sci.: Polym. Phys.*, 1987, **25**, 717.
17. Brandrup, J. and Immergut, E. H., *Polymer Handbook*, 3rd edn. John Wiley, New York, 1989.
18. Loufakis, K. and Wunderlich, B., *Macromolecules*, 1987, **20**, 2474.